

Preparation and characterization of titanium dioxide nanocomposite fibers

Qufu Wei · Liangyan Yu · Robert R. Mather ·
Xueqian Wang

Received: 24 September 2006 / Accepted: 5 February 2007 / Published online: 26 June 2007
© Springer Science+Business Media, LLC 2007

Abstract Titanium dioxide and polypropylene fibers were prepared by melt-compounding and sputter coating, respectively. Energy dispersive x-ray analysis (EDX) confirmed the presence of titanium dioxide in the fibers. Through the application of environmental scanning electron microscopy (ESEM) and scanning probe microscopy (SPM), it was found that incorporating the titanium dioxide by melt-compounding caused severe aggregation of the titanium dioxide nanoparticles at the polypropylene fiber surface. Indeed, coverage of the fiber surface by titanium dioxide was poor. By contrast, the coverage of the sputter coated fiber surfaces was much more consistent, although aggregation of the titanium dioxide nanoparticles still appeared quite extensive. The behavior of the nanocomposite fiber surfaces was investigated using dynamic contact angle measurements by the Wilhelmy technique. Only a small increase in hydrophilicity of the polypropylene fibers was observed after melt-compounding with titanium dioxide, but a larger increase was noted after sputter coating. UV irradiation appreciably enhanced the hydrophilicity of the fiber surfaces in both cases.

Introduction

It is by now well established that textile fibers containing additives, especially additives incorporated in dimensions of a nanoscale, show great potential for a wide variety of applications. One such additive that has attracted considerable commercial attention is titanium dioxide. Indeed, titanium dioxide has been used as a delustrant in synthetic fibers for a long time, and it is well known as a white pigment. However, the development of titanium dioxide particles that is smaller than those used in pigment formulations has opened up other potential applications for it. Titanium dioxide is interesting in terms of its optical, electronic and UV-absorbing properties and shows promise for a variety of applications, including self-cleaning, UV blocking, purification and antibacterial applications [1–3].

The textile industry too stands to benefit from the special properties of titanium dioxide. Thus, the decomposition of trichloroethylene in a photoreactor with a titanium dioxide coated terephthalic acid (PTA) nonwoven textile has been reported [4]. The surface coating of electrospun polymer fibers by titanium dioxide using sol–gel technology has also been reported [5]. Titanium dioxide nanoparticles can also be added to textiles by chemical vapor deposition [6].

It is evident that the distribution of the titanium dioxide particles within a fiber will be important. A number of melt-processing fiber producing industries still prefer to mix all the additives that they consider are required right at the start of processing; these additives are mixed with polymer granules before the extrusion process. The additives are, therefore, distributed throughout the bulk of the fibers. The uniformity of distribution depends on the effectiveness of the mixing process before extrusion and also on the extent to which the particles have aggregated during mixing and extrusion.

Q. Wei (✉) · L. Yu
Key Laboratory of Eco-textiles of Ministry of Education,
Southern Yangtze University, Wuxi 214122, China
e-mail: qfwei@sytu.edu.cn

R. R. Mather
School of Engineering and Physical Sciences, Heriot-Watt
University, Edinburgh EH14 4AS, Scotland, UK

X. Wang
Anhui University of Technology and Science, Wuhu 214000,
China

A major problem with handling particles of nanoscale dimensions is the high tendency of such particles to aggregate. This propensity for aggregation arises from the high ratio of surface area to volume in each particle and is further promoted by roughness in the particle surface. A high interfacial energy between the particles and the fiber matrix will also lead to particle aggregation. In addition, the additive may be required only at the fiber surface, rather than being distributed within the fiber bulk.

This paper describes some initial work on the characterization of titanium dioxide nanocomposite polypropylene fibers, prepared by melt-compounding and sputter coating. The fiber surfaces were observed using both environmental scanning electron microscopy (ESEM) and scanning probe microscopy (SPM). Wetting properties of the fibers were also assessed.

Materials and methods

Materials

The grade of titanium dioxide was P-25 from Degussa, used as received without further treatment. The grade consists of 75% of the anatase crystal form and 25% of the rutile form. The cross-sectional dimension of the P-25 particles is ca. 30 nm. The type of polypropylene resin used was HF445J B2-9037 from Borealis. The melt flow index of the resin is 19.0 g/10 min.

Melt-compounding

The polypropylene granules were milled into powders and mixed with the titanium dioxide nanoparticles in a tumbler mixer for 30 min. The nanocomposite fibers were processed at 230 °C from pilot-plant scale melt-extrusion equipment, supplied by Extrusion Systems Ltd., UK. The equipment has been described elsewhere [7]. There were three heating zones in the barrel of the extruder, one in the metering pump and two in the die head, which contained a filter package and the spinneret. The extruded filament was cooled in a flow of ambient side-blown air in a quenching chamber. The drawdown ratio was ca. 100. No spin finish was applied. The spinning conditions are given in Table 1.

Sputter coating

An RF sputter coating system was used to deposit a nanofilm of titanium dioxide on pure polypropylene fibers, spun using the conditions shown in Table 1. A high-purity titanium dioxide target was used. The background pressure of the system was less than 10^{-5} Pa. A mixture of argon and oxygen (95:5) was used as the sputter gas. The depositions

Table 1 Fiber spinning conditions

Zone 1 temperature (°C)	215
Zone 2 temperature (°C)	225
Zone 3 temperature (°C)	230
Spinning temperature (°C)	230
Number of spinneret holes	55
Hole size of spinneret (mm)	0.4
Metering pump capacity ($\text{cm}^3 \text{rev}^{-1}$)	2.4
Metering pump speed (rev min^{-1})	3
Winding speed (m min^{-1})	100
Cold draw ratio	2:1

were conducted at a total pressure of 8×10^{-1} Pa. The distance between the target and the substrates was kept at 80 mm. The sputtering was performed for 60 min.

Surface morphology

The surface morphology was examined by scanning probe microscopy, using a SPM 4000 microscope, produced by Benyuan, China. Scanning was carried out in contact mode SPM. All images were obtained under ambient conditions.

EDX analysis

A Philips XL30 ESEM-FEG equipped with a Phoenix energy dispersive x-ray analysis system (EDX) was used to examine the chemical compositions of the nanocomposite fibers. An accelerating voltage of 20 kV was applied over a period of 100 s.

Dynamic contact angles

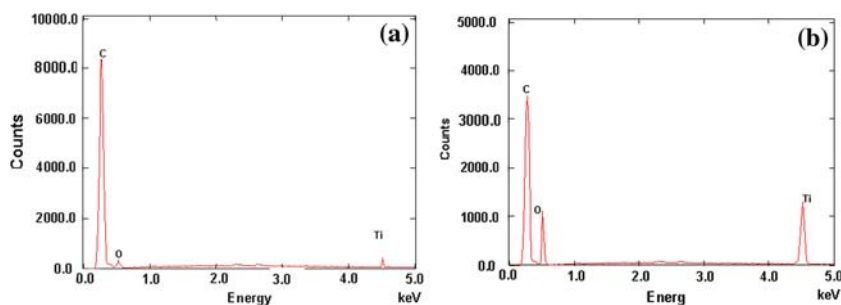
The wetting properties of the nanocomposite fibers were examined by determining the contact angles of water along the lengths of the fibers. Advancing and receding dynamic contact angles for an individual fiber were determined at 20 °C by the Wilhelmy technique [8] using a CDCA-100F instrument produced by Camtel Ltd., UK. Fibers which had been subjected to 2 h of UV (ultra violet) illumination at 315 nm were compared with corresponding fibers, which had received no illumination. In this test, distilled water was used.

Results and discussion

EDX analysis

Figure 1a shows the EDX spectrum for the melt-compounded nanocomposite fibers, and Fig. 1b shows the EDX spectrum for the sputter coated nanocomposite fibers.

Fig. 1 EDX spectrum of TiO₂/PP nanocomposite fiber (a) extruded and (b) sputter coated



For both types of nanocomposite fiber, peaks corresponding to oxygen and titanium are revealed. It is noteworthy that the oxygen and titanium peaks are much more intense relative to the carbon peak for the sputter coated fibers than for the melt-compounded fibers. This observation can be explained by the greater proportion of titanium dioxide on the fiber surfaces of the sputter coated fibers.

Surface morphology

Figure 2 shows images of the morphology of the untreated polypropylene fibers. The SPM images reveal the fiber surface to be quite smooth. The nanofibril structures on the fiber surface are observed in the SPM image (Fig. 2), which has a higher magnification, to possess cross-sections ranging from ca. 50 nm to 200 nm.

The image in Fig. 3 shows image of the melt-compounded nanocomposite fibers. The SPM image (Fig. 3) clearly indicates the presence of some titanium dioxide particle assemblies embedded in the polypropylene fibers. The size of these assemblies is up to ca. 150 nm, or even a little higher. This is approximately five times the size of the discrete titanium dioxide nanoparticles (ca. 30 nm). There are, therefore, about 5³ nanoparticles in each assembly. The size of the assembly is over 100 times that of its constituent nanoparticles. Clearly, then, there is severe aggregation of the nanoparticles at the fiber surface. There is the suggestion too from the SPM image (Fig. 3)

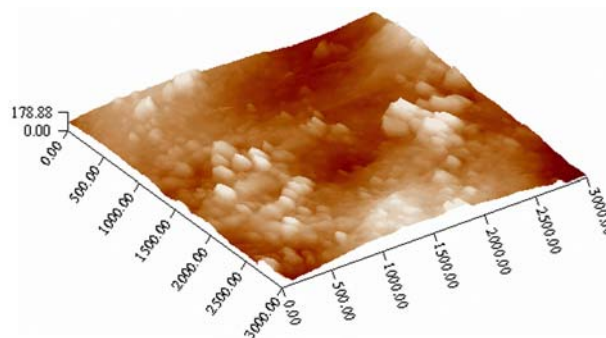


Fig. 3 SPM image of TiO₂/PP Nanocomposite fiber prepared by melt-compounding

that not only is their extensive particle aggregation, but also the aggregate sizes vary widely, and the aggregates are not uniformly distributed over the fiber surface. The aggregates themselves may be further aggregated.

Figure 4 shows image of the nanocomposite fiber morphology after sputter coating with titanium dioxide. In contrast to the SPM image in Fig. 3, the image in Fig. 4 reveals no nanofibrils on the fiber surface. There is, however, evidence of the presence of titanium dioxide nanoparticles, revealed in the corresponding SPM image (Fig. 4). Sputter coating appears to produce much more extensive and uniform coverage of the fiber surface, although the size of each cluster of titanium dioxide is still notably larger than 30 nm, the size of a discrete nanoparticle. Thus, a more even

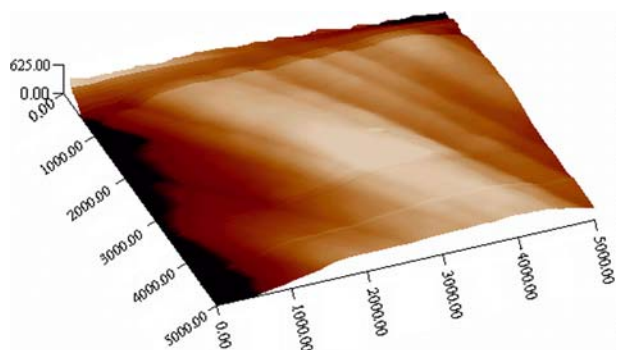


Fig. 2 SPM image of PP fiber

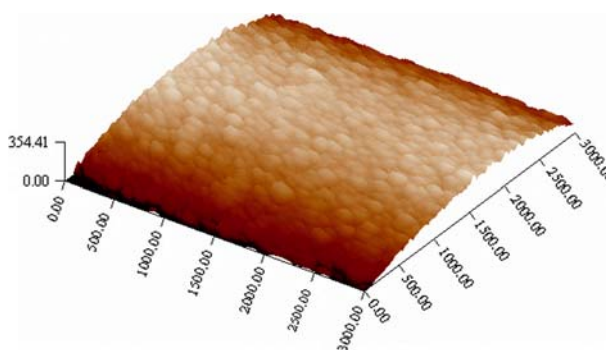


Fig. 4 SPM image of sputter coated fiber

distribution of the titanium dioxide nanoparticles on the fiber surface is obtained from sputter coating than from melt-compounding. However, even after sputter coating, the nanoparticles appear aggregated to some degree.

Dynamic contact angles

Figure 5 shows dynamic contact angles of water on the melt-compounded fibers before and after UV irradiation at 315 nm for 2 h. The variations of advancing and receding contact angles along a fiber length of ca. 3 mm can be seen from the figure. For the melt-compounded nanocomposite fiber, an advancing contact angle of 90–95° is found. The receding contact angle is about 70°. The difference of 20–25° between the advancing and receding contact angles can be attributed to the roughness of the fiber surface, as revealed in Fig. 3.

The contact angles for pure polypropylene fibers are about 98° [9]. These values are only slightly higher than for the melt-compounded fibers, and therefore, also show that the coverage of the melt-compounded fibers by titanium dioxide is poor. After UV irradiation, the advancing contact angle fall to ca. 75°, and the receding contact angle to 55°. The wetting character of the nanocomposite fiber has been improved by its exposure to UV radiation.

Figure 6 shows dynamic contact angles of water on the sputter coated fibers. The advancing and receding contact angles are found to be ca. 85° and 70°, respectively. Thus, the advancing contact angle is lower than for the melt-compounded fibers, but the receding contact angle has about the same value. The difference between the advancing and receding contact angles is ca. 15° and, therefore, lowers than for the melt-compounded fibers. The smaller difference may be attributable to less roughness on the surface of the sputter coated fibers, a consequence perhaps of the more consistent layer of titanium dioxide on the fiber surface (Fig. 4). Both contact angles are considerably lowered as a result of UV irradiation to ca. 50° and 35°, respectively. The fiber surfaces have become much

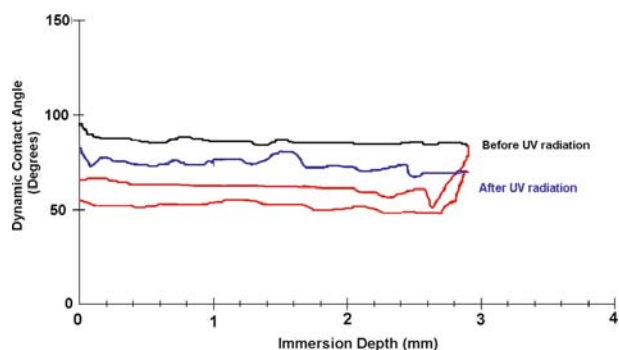


Fig. 5 Dynamic contact angles of extruded TiO₂/PP nanocomposite fiber

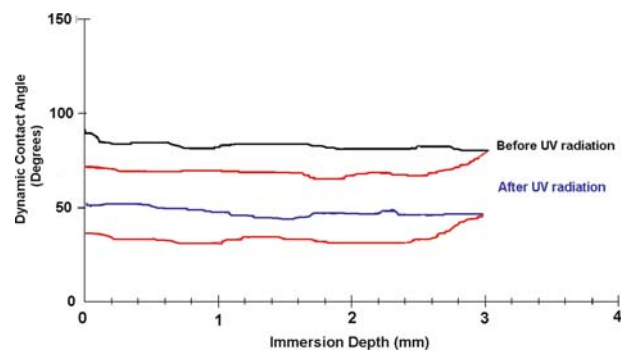


Fig. 6 Dynamic contact angles of sputter coated TiO₂/PP nanocomposite fiber

more hydrophilic. This is attributed to the photocatalytic behavior of titanium dioxide, which has a bandgap energy of 3.2 eV (corresponding to 400 nm UV) and generates free radicals by UV radiation. [10]

Conclusions

This paper uses titanium dioxide in polypropylene fibers as an example to illustrate that great care is needed in order to obtain an even distribution of nanoparticles, whether it is within the bulk of a fiber or on its surface. Of the two methods used to incorporate titanium dioxide nanoparticles into polypropylene fiber, melt-compounding caused the nanoparticles to be highly aggregated, and coverage of the fiber surface with titanium dioxide was poor. The coverage of the sputter coated polypropylene fiber surfaces by titanium dioxide was much better, although the nanoparticles still appeared quite extensively aggregated.

The behavior of the treated fiber surfaces was explored through dynamic contact angle measurements. The hydrophilic nature of the fiber surfaces was only slightly increased by melt-compounding, an observation providing further evidence of their poor coverage by the titanium dioxide nanoparticles. Hydrophilicity was increased much more after sputter coating, as would be expected from better surface coverage by titanium dioxide. UV irradiation appreciably enhanced the hydrophilic surface nature in both cases.

Acknowledgment This work was supported by the Key Project of the Chinese Ministry of Education (No. 106089) and the Program for New Century Excellent Talents in University (NCET-06-0485).

References

1. Fujishima A, Rao TN, Tryk DA (2000) *J Photochem Photobiol C Photochem Rev* 1:1
2. Yang H, Zhu S, Pan N (2004) *J Appl Polym Sci* 92:3201

3. Daoud WA, Xin JH, Zhang YH (2005) Surf Sci 599:69
4. Ku Y, Ma CM, Shen YS (2001) Appl Cat B Environmental 34:181
5. Caruso RA, Schattka JH, Greiner A (2001) Adv Mater 13:1557
6. Parkin IP, Palgrave RG (2005) J Mater Chem 15:1689
7. Yang RD, Mather RR, Fotheringham AF (1999) Int Polym Processing 14:60
8. Krishnan A, Liu YH, Cha P, Woodward R, Allara D, Vogler EA (2005) Colloid Surface B 43:95
9. Gupta BS, Whang HS (1999) Int Nonwovens J 8:91
10. Friesen DA, Morello L, Headley J, Langford CH (2000) J Photochem Photobiol A: Chem 133:213